Body wall development in lamprey and a new perspective on the origin of vertebrate paired fins

Frank J. Tulenko[a], David W. McCauley[b], Ethan L. MacKenzie[a], Sylvie Mazan[c], Shigeru Kuratani[d], Fumiaki Sugahara[d], Rie Kusakabe[e], and Ann C. Burke[a,1]

[a]Department of Biology, Wesleyan University, Middletown, CT 06459; [b]Department of Biology, University of Oklahoma, Norman, OK 73019; [c]Centre National de la Recherche Scientifique – Université Pierre et Marie Curie UMR 7150, Development and Evolution of Vertebrates Group, Station Biologique, 29688 Roscoff, France; [d]Laboratory for Evolutionary Morphology, RIKEN Center for Developmental Biology, Kobe 650-0047, Japan; and [e]Department of Biology, Graduate School of Science, Kobe University, Kobe 657-8501, Japan

Edited* by Neil H. Shubin, University of Chicago, Chicago, IL, and approved June 4, 2013 (received for review March 5, 2013)

Classical hypotheses regarding the evolutionary origin of paired appendages propose transformation of precursor structures (gill arches and lateral fin folds) into paired fins. During development, gnathostome paired appendages form as outgrowths of body wall somatopleure, a tissue composed of somatic lateral plate mesoderm (LPM) and overlying ectoderm. In amniotes, LPM contributes connective tissue to abaxial musculature and forms ventrolateral dermis of the interlimb body wall. The phylogenetic distribution of this character is uncertain because lineage analyses of LPM have not been generated in anamniotes. We focus on the evolutionary history of the somatopleure to gain insight into the tissue context in which paired fins first appeared. Lampreys diverged from other vertebrates before the acquisition of paired fins and provide a model for investigating the preappendicular condition. We present vital dye fate maps that suggest the somatopleure is eliminated in lamprey as the LPM is separated from the ectoderm and sequestered to the coelomic linings during myotome extension. We also examine the distribution of postcranial mesoderm in catshark and axolotl. In contrast to lamprey, our findings support an LPM contribution to the trunk body wall of these taxa, which is similar to published data for amniotes. Collectively, these data lead us to hypothesize that a persistent somatopleure in the lateral body wall is a gnathostome synapomorphy, and the redistribution of LPM was a key step in generating the novel developmental module that ultimately produced paired fins. These embryological criteria can refocus arguments on paired fin origins and generate hypotheses testable by comparative studies on the source, sequence, and extent of genetic redeployment.

Paired fins were a key novelty that arose early in the radiation of vertebrates, changing locomotor ability and ecological opportunity. Historically, two hypotheses for the evolutionary origin of paired fins have generated the most discussion: the gill arch hypothesis (1) and the lateral fin fold hypothesis (2–4). The gill arch hypothesis posits that paired fins arose through transformation of the posterior gill skeleton. The lateral fin fold hypothesis maintains that paired fins evolved as retained portions of a continuous lateral fin structurally similar to the median fin observed in anamniote embryos. Neither hypothesis in its original formulation is well-supported by either the fin morphologies of stem gnathostomes or the developmental morphologies of extant taxa (5–8). Recent studies have explored generative homologies to gain insight into how paired appendages evolved and have shown that several of the genes that pattern paired fins/limbs also function during the development of gill arches [sonic hedgehog and fibroblast growth factor 8 (9)], median fins [*Hox9–13*, *T-box18*, and fibroblast growth factors (10–12)], and the heart field [*T-box4/5* (13–15)]. Notably, these data are consistent with aspects of both the gill arch and lateral fin fold hypotheses and support the argument that the evolution of paired fins involved the redeployment of preexisting patterning programs into a new embryonic context (i.e., the fin-forming fields) (16, 17). Implicit in both classical and recent discussions of the origin of the appendicular system is the presence of undifferentiated precursor tissue in which evolution produced paired fins. We address a neglected aspect of this discussion by focusing on the nature of the ancestral body wall in which paired fins evolved.

The musculoskeletal body plan of ancestral vertebrates consisted of branchial and axial structures only, including gills supported by skeletal arches, segmental myotomes, and median fins (18, 19). In extant gnathostomes, paired appendages appear as additions to an embryo that has already developed an axial body plan. Vertebrae, ribs, and segmental myotomes comprise the axial musculoskeletal system and derive from somitic mesoderm. Fin/limb buds appear at pectoral and pelvic levels as outgrowths of the somatopleure, and signaling between the ectoderm and somatic lateral plate mesoderm (LPM) is critical for their formation (20). Somitic myoblasts infiltrate these buds to form appendicular musculature (21).

Lampreys are agnathan vertebrates that split from the lineage, leading to gnathostomes before the origin of paired fins (22, 23). Although their suitability as a proxy for the ancestral condition of more derived vertebrates is a matter of continuing debate (24, 25), lamprey embryos provide the best option for exploring the embryological context in which paired fins arose and testing hypotheses about the distribution of LPM in early gnathostomes. Recent studies have shown that the lamprey myotome is dorsoventrally compartmentalized, despite lacking a horizontal septum (26), and that the LPM is patterned into distinct cardiac and posterior regions (14, 15). Few studies, however, have characterized the lamprey LPM during stages of body wall formation (15, 27). Here, we examine the morphological changes taking place during this process in both the Sea Lamprey *Petromyzon marinus* and the Japanese Lamprey *Lethenteron japonicum* to extend classical descriptions (28–30) and provide long-term fate maps of somitic and LPM in an agnathan vertebrate. Additionally, we performed antibody labeling in the shark *Scyliorhinus canicula* and isotopic mesoderm transplants in axolotl to visualize the interface between somitic and LPM in two major gnathostomes lineages.

Results

Histological Anatomy in Lamprey Embryos. Histological anatomy during body wall formation is very similar in *P. marinus* and *L. japonicum* (Figs. 1 *A* and *B* and 2 and Fig. S1). In plastic sections of early stage embryos (stage 23) (31), the presumptive LPM (PLPM) forms a thin layer of cells that extends laterally from the somites, separating the dorsal epidermis from the underlying endoderm (Fig. 1 *A* and *B* and Fig. S1 *A* and *B*). During subsequent stages of development (stages 24–30), the embryo straightens, the yolk ball elongates into a tube, and new

Author contributions: F.J.T. and A.C.B. designed research; F.J.T., E.L.M., and F.S. performed research; D.W.M., S.M., S.K., and R.K. contributed new reagents/analytic tools; F.J.T., E.L.M., and A.C.B. analyzed data; and F.J.T. and A.C.B. wrote the paper.

The authors declare no conflict of interest.

*This Direct Submission article had a prearranged editor.

[1]To whom correspondence should be addressed. E-mail: acburke@wesleyan.edu.

This article contains supporting information online at www.pnas.org/lookup/suppl/doi:10.1073/pnas.1304210110/-/DCSupplemental.

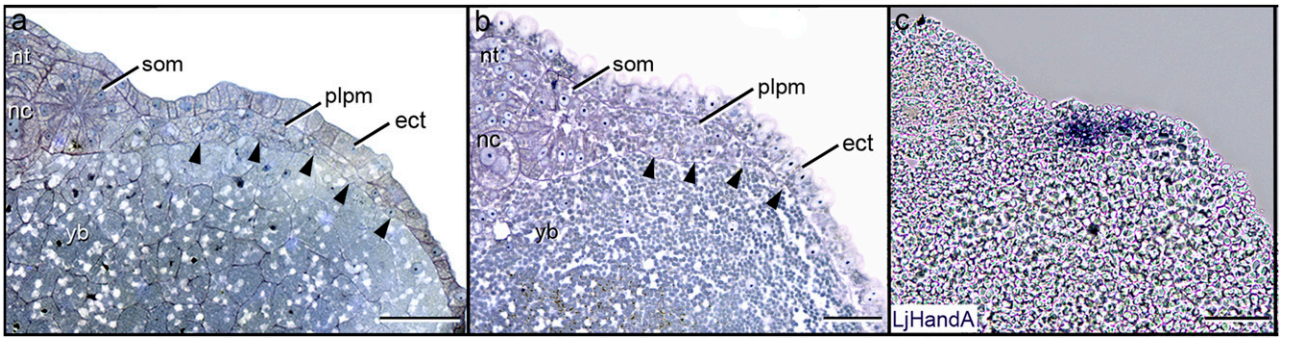

Fig. 1. Distribution of LPM in stage 23/24 lamprey embryos. (*A* and *B*) Plastic sections through the midyolk ball of (*A*) *Petromyzon* and (*B*) *Lethenteron* embryos stained with toluidine blue. In both *A* and *B*, PLPM (plpm) extends laterally from the somites (som) along the dorsum of the yolk ball (yb). (*C*) Cryosection of whole mount in situ of *Lethenteron* embryo. Expression of *LjHandA* (blue) supports lateral plate identity of PLPM. Fig. S3 shows additional stages. ect, ectoderm; nc, notochord; nt, neural tube. (Scale bar: 50 μm.)

myotomes form from somitic mesoderm in an anterior to posterior direction (Fig. S2). The PLPM in these later stages first surrounds the yolk tube (Fig. 2 *A* and *D* and Fig. S1 *C* and *D*) and then splits into distinct somatic and splanchnic layers well before myotome closure of the body wall (Fig. 2 *E*, *F*, and *H* and Fig. S1 *E–H*). The dermomyotome (DM), a thin layer of undifferentiated cells on the external surface of the myotome, forms distinct lip-like folds both dorsally and ventrally (Fig. 2 *A*, *B*, *E*, and *F* and Fig. S1 *C–F*). As the ventral lip of the DM advances, it appears to wedge between the ectoderm and the somatic layer of the PLPM (Fig. 2 *E* and *F* and Fig. S1 *E* and *F*).

Molecular Identification of Embryonic Populations in Lamprey. The transcription factor dHand has been used as a molecular marker of early LPM in a number of vertebrate taxa, including lamprey (8, 15, 32, 33). We performed whole-mount in situ hybridization for *LjHandA* in *Lethenteron* embryos. As previously reported, *LjHandA* is expressed in the branchial region and heart as well as the PLPM of *Lethenteron* embryos at stages 23–27 (Fig. S3). We confirmed the position of label within the PLPM in cryosections (Fig. 1*C* and Fig. S3 *E, G,* and *I*), supporting the lateral plate (LPM) identity of this tissue. As development proceeds, the expression domain of *LjHandA* extends ventrally to surround the yolk tube (stage 25) (Fig. S3 *B–D* and *F*), consistent with the early ventral migration of LPM (compare Fig. 2 *A* and *D* with Fig. S3*F*). *LjHandA* in the LPM is then down-regulated in an A–P sweep as the myotomes extend ventrally, and becomes limited to the posteriormost region of the embryo by stage 27. In the absence of gene expression at stages of myotome extension, the distribution of LPM cells is difficult to follow, although as mentioned above, a thin layer of cells is visible in plastic section deep to the myotome and between the ectoderm and yolk (Fig. 2 *A*, *B*, and *D–F* and Fig. S1 *C–F*). Probes generated from partial sequence of *Petromyzon Hand* labeled heart and branchial regions but did not show strong LPM label.

Pax3/7 transcription factors are established markers for the DM in vertebrates (26, 34, 35). We used the antibody DP312, which recognizes Pax3/7 proteins (36, 37), to visualize changes in the position of the DM in lamprey embryos at different stages of development. In *Petromyzon*, DP312 labeling of the ventral lip of the DM (Fig. 2 *B*, *C*, *F*, and *G*) makes visible the ventral

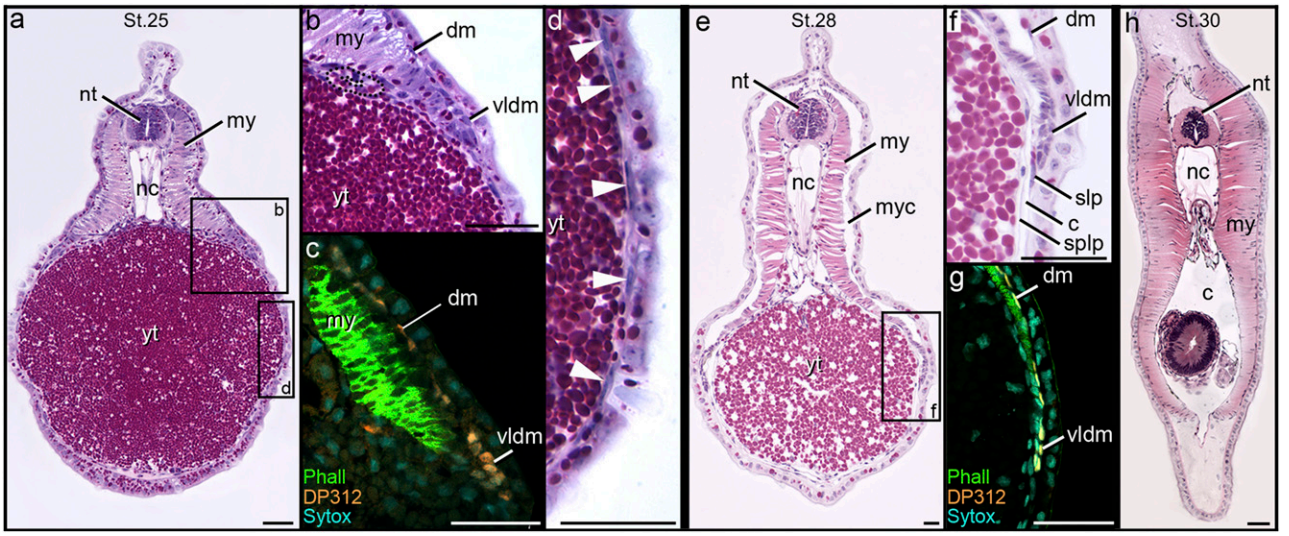

Fig. 2. Plastic sections and DP312 labeling of *Petromyzon* embryos and larvae. (*A*, *B*, *D–F*, and *H*) Plastic sections stained with H&E. (*C* and *G*) Cryosections are labeled for Pax3/7 (orange; DP312), skeletal muscle (green; phalloidin), and nuclei (cyan; Sytox). (*A–D*) Stage 25. DP312-positive cells of the DM (dm) are adjacent to the inner surface of the ectoderm and form an epithelial lip ventrally (vldm; compare *B* with *C*). Elongate cells of the presumptive LPM (arrowheads in *D*) surround the yolk tube (yt). (*E–G*) Stage 28. The LPM has split into somatic (slp) and splanchnic (splp) layers, forming a coelom (c). (*E–G*) The ventral lip of the dermomyotome is positioned between ectoderm and somatic lateral plate. (*H*) Stage 30. Myotomes close the body wall ventrally. Fig. S2 shows approximate planes of section. my, myotome; myc, myocoel; nc, notochord; nt, neural tube. (Scale bar: 50 μm.)

migration of the somitic tissue as it extends between the ectoderm and underlying tissue during body wall closure.

DiI Labeling of Mesoderm in the Lamprey Body Wall. We further characterized the interface of somitic and lateral plate tissue in lamprey by injecting the vital dye DiI into either somites or LPM of young *Petromyzon* embryos, which allowed long-term fate mapping of cells within these populations (stages 22–24) (Fig. 3 and Figs. S4 and S5). In total, we performed 188 somite and 209 LPM injections, which were then collected either within 12 h of injection to evaluate DiI targeting or at developmental stages with varying degrees of body wall closure (stages 25–30) (Table S1). We sectioned embryos with the brightest whole-mount fluorescence (18 somite injections; 29 LPM injections) (Table S1) and stained sections from older embryos for skeletal muscle. Results of injections were consistent across specimens (Tables S2 and S3), and sections of embryos collected within 12 h of injection showed localization of DiI in targeted tissue (Fig. 3 *A* and *B*).

In whole mounts of somite-injected embryos, the distribution of DiI is largely coincident with a single myotome (Fig. S4). Cross-sections show DiI-positive myofibers and labeled cells in the DM and presumptive sclerotome as well as rare mesenchymal cells within the dorsal fin fold (Fig. S4 *D–H* and Table S3). In a majority of embryos at stages 25–28 (10/14) (Table S3), DiI-labeled cells are present in the ventral lip of the DM (compare Fig. S4 *F* and *H* with Fig. 2 *B*, *C*, *F*, and *G*). No migratory DiI-positive cells are present ventral to this lip in any somite-injected embryos examined, indicating that the ventral lip of the dermomyotome is the leading edge of somitic mesoderm during body wall closure.

In LPM-injected embryos, DiI-positive cells form a band of labeled tissue largely restricted to the ventral one-half of each specimen (Fig. 3 *C–E*). Cross-sections through stage 25/26 embryos reveal the movement of DiI-positive cells from the dorsum of the yolk ball to surround the yolk tube (Fig. 3 *C–G*), consistent with changes in histology (Fig. 2*D*) and lamprey *Hand* expression as described above (Fig. S3 *A–C* and *F*). In more advanced embryos, DiI-positive cells are observed medial to the myotome but not within the myotome or lateral to it (Fig. 3 *H* and *I*, Fig. S5 *A–E*, and Table S3), with the exception of labeled ectoderm at the injection site. By the larval stage (stage 30), DiI-positive cells contribute to the coelomic linings, typhlosole, and gut vasculature (Fig. 3 *J* and *K* and Fig. S5 *F–K*).

Mesoderm Distribution in Catshark Pectoral Fin and Body Wall. We used the antibody DP312 to label the dermomyotome of the catshark *S. canicula*, a galeomorph shark belonging to the order Carcharhiniformes (38). In stage 27 embryos (39), the pectoral fin buds are present as ventral expansions of the somatopleure (Fig. 4 *A* and *B*). In cross-section, the DP312-labeled DM closely opposes the ectoderm dorsally. The ventral lip of the DM, however, loses contact with the modified ectoderm of the fin bud at the approximate level of the nephric duct and enters the fin bud mesenchyme (LPM) (Fig. 4 *A* and *B*). At interfin levels of the same stage, no mesenchymal cells separate the DM and ectoderm (Fig. 4 *C* and *D*). In contrast, in interfin sections of stage 28 embryos, the DM loses contact with the ectoderm, and loose mesenchyme separates the two tissues (Fig. 4 *E* and *F*). A distinct boundary is visible at the level of the nephric duct between the DP312-positive mesenchyme generated from the DM and the DP312-negative mesenchyme (Fig. 4 *E* and *F*). We interpret this label-boundary as the lateral somitic frontier, the interface of somitic and LPM tissues (40). The mesenchyme and ectoderm ventral to this boundary comprise the somatopleure, which persists in the external body wall.

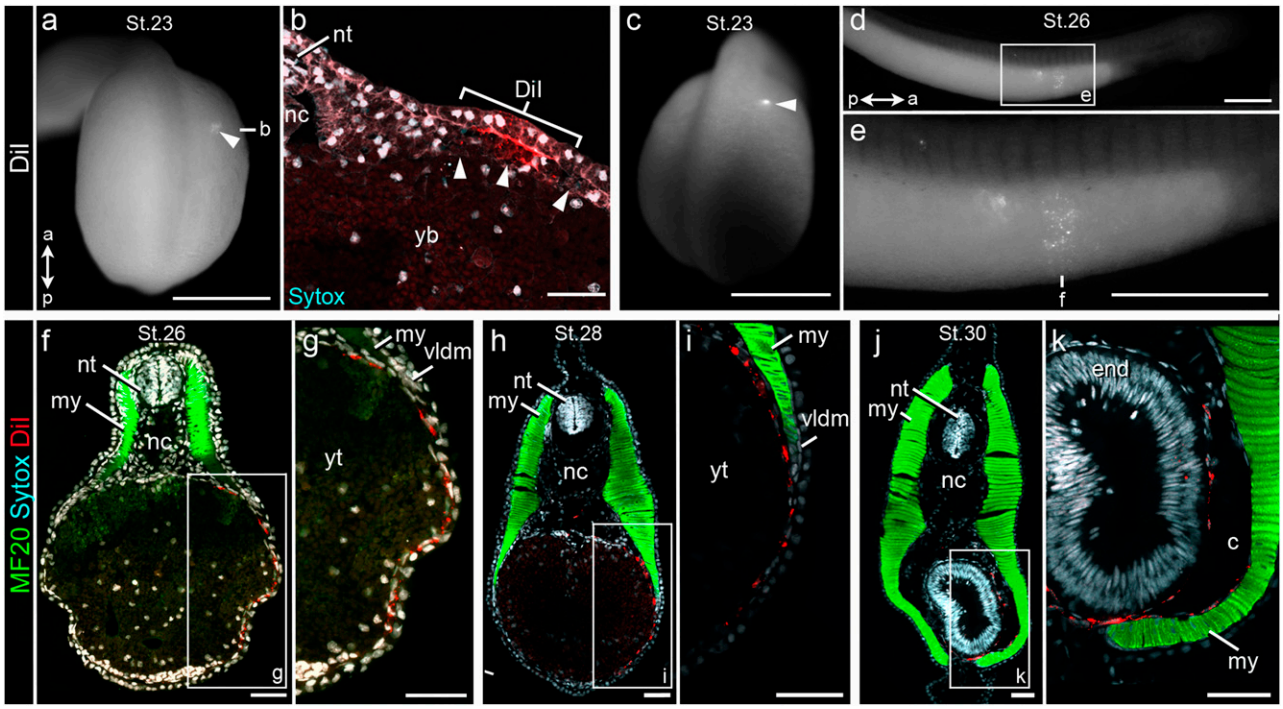

Fig. 3. DiI labeling of LPM in *Petromyzon*. (*A*) Dorsal view of stage 23 embryo at time of injection (arrowhead indicates position of DiI). (*B*) Cryosection through same embryo showing DiI (red) in targeted LPM (arrowheads). (*C*) Dorsal view of stage 23 embryo at time of injection (arrowhead indicates position of DiI), and (*D* and *E*) lateral view of same embryo at stage 26. (*F–K*) Cryosections through (*F* and *G*) LPM-injected embryo shown in *C–E* and embryos at (*H* and *I*) stages 28 and (*J* and *K*) 30 labeled for skeletal muscle (green; MF20) and nuclei (cyan; Sytox). DiI-positive cells (red) surround the yolk tube by stage 26 and contribute to the coelomic linings by stage 30. Note that DiI-positive cells are always medial or ventral to the myotome (my) and never lateral to or within the my (Fig. S5). Fig. 2 defines abbreviations. end, endoderm. (Scale bar: 50 μm.)

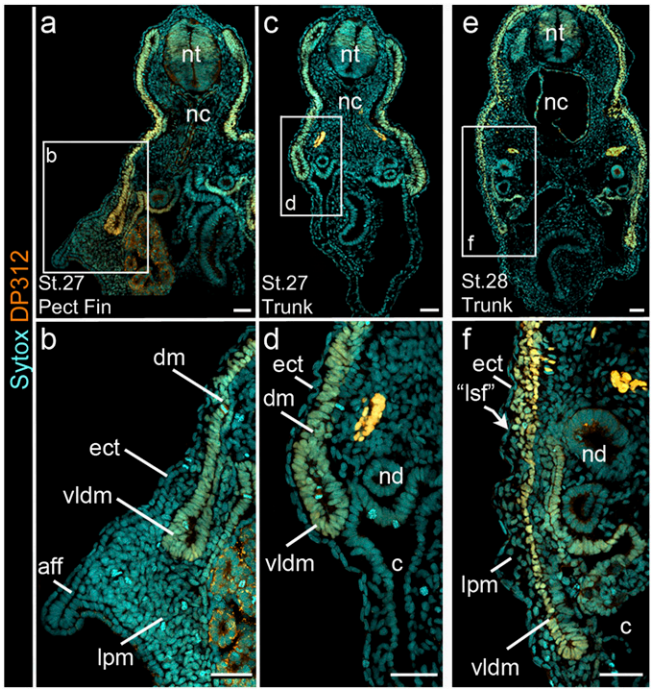

Fig. 4. DP312 labeling in *Scyliorhinus*. (*A*–*D*) Cryosections through (*A* and *B*) the pectoral fin and (*C* and *D*) interfin trunk of stage 27 catshark. (*A* and *B*) Mesenchyme is present between the DP312-positive DM (dm; orange) and modified ectoderm of the fin bud. In contrast, mesenchymal cells are not seen (*A* and *B*) between the DP312-positive dm and ectoderm (ect) dorsal to the fin bud or (*C* and *D*) along the interfin trunk at this stage. (*E* and *F*) Cryosections through the interfin trunk of a stage 28 catshark. At the level of the nephric duct (nd), DP312-positive mesenchyme from the dermomyotome forms a boundary with unlabeled mesenchyme from presumptive lateral plate. aff, apical fin fold; "lsf," lateral somitic frontier. Fig. 2 defines abbreviations. (Scale bar: 50 μm.)

Lateral Plate Transplants in Axolotl Embryos. We examined the distribution of somatopleure in axolotls (*Ambystoma mexicanum*) by isotopically transplanting LPM and ectoderm from GFP donors to WT hosts. Pronephros was included in a subset of grafts to ensure transplantation of the dorsal margin of LPM (Fig. 5 *A*–*C* and Fig. S6 *A* and *B*). In total, we performed 42 surgeries and sectioned 10 of these surgeries between stages 32 and 57 (41, 42) (Table S4). Sections of chimeras collected 1 d postoperative revealed well-incorporated graft (Fig. S6 *C* and *D*). In whole mounts of chimeras reared to stages 46–57, graft-derived cells contribute to both the fore- and interlimb regions. Sections through the pectoral region reveal GFP-positive cells forming connective tissue of appendicular musculature (e.g., dorsalis scapulae and pectoralis) and the hypaxial myotome as well as chondrocytes of the pectoral girdle (scapula and coracoid) (Fig. 5 *D*–*E*′). At interlimb levels, myofibers of the hypaxial myotome are also invested by GFP-positive cells. The LPM of the somatopleure is visible as GFP-positive mesenchyme lateral to the muscular body wall (Fig. 5 *F*–*G*′).

Discussion

Persistence of the Somatopleure in Gnathostome. Our results provide evidence suggesting that the distribution of mesodermal lineages in the body wall of lamprey differs significantly from the body wall of gnathostomes. The histological, gene expression, and fate mapping data shown here indicate that, in lamprey, the LPM extends around the yolk tube before ventral advance of somitic mesoderm and that the ventral lip of the dermomyotome extends along the inner surface of the ectoderm, displacing the LPM inward during myotome closure of the body wall. In the absence of a permanent molecular marker for the somatic lateral plate, our DiI-labeling experiments strongly suggest that the somatopleure, which is present in the early embryo, is eliminated during this process, because LPM is segregated to the coelomic linings.

In model amniotes, it is well-established that LPM contributes connective tissue to both the musculature (e.g., latissimus dorsi and abdominal obliques) and superficial dermis of the flank, thus reflecting a somatopleure contribution to the adult body wall (40, 43, 44). The phylogenetic distribution of this character has been uncertain in the absence of lineage analyses in anamniotes. Our isotopic transplants of early LPM from GFP axolotls into WT hosts show that the salamander body wall includes LPM cells medial and lateral to as well as within body wall musculature. These data also indicate that an abaxial body wall is likely primitive for tetrapods.

Considering the evolutionary transition from fins to limbs, it would seem possible that the persistence of the somatopleure reflects morphological changes at the base of the tetrapod radiation or during the transition to a terrestrial environment. Chondrichthyans can be used as an outgroup to test this hypothesis. They are the sister group of all other living gnathostomes,

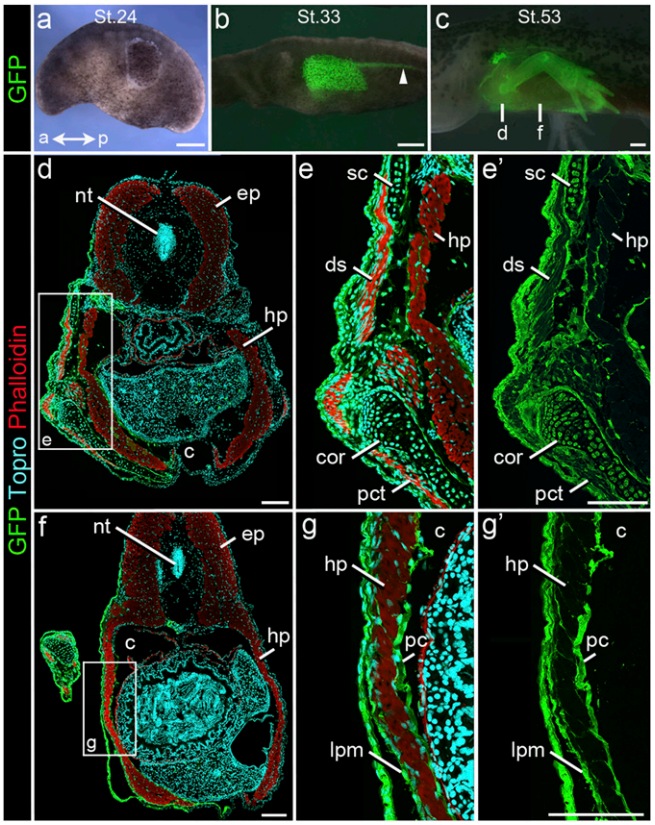

Fig. 5. GFP to WT Isotopic transplants of LPM/Pronephros/Ect in *Ambystoma*. (*A*–*C*) Lateral view of a surgery chimera at (*A*) stage 24 (time of surgery) and the same specimen at (*B*) stages 33 and (*C*) 53, showing distribution of GFP donor tissue (green). Note (*B*) caudal migration of pronephros (arrowhead) and (*C*) graft-derived skeletal elements of the forelimb. (Scale bar: 500 μm.) (*D*–*G*′) Cryosections through (*D*–*E*′) the pectoral and (*F*–*G*′) the interlimb regions of larva pictured in *C* labeled for GFP (green), skeletal muscle (red; phalloidin), and nuclei (cyan; TO-PRO). (*D*–*E*′) In the pectoral region, graft-derived cells are present in scapula (sc) and coracoid (cor) and form the connective tissue of appendicular muscles (ds, dorsalis scapulae; pct, pectoralis) and the hypaxial myotome (hp). (*F*–*G*′) In interlimb levels, graft-derived cells form mesenchyme lateral to hp as well as connective tissue within hp. ep, epaxial myotome; pc, parietal coelomic lining. Fig. 2 defines abbreviations. (Scale bar: 250 μm.)

and their embryos can be used to gain insight into the development of the last common ancestor of all vertebrates with paired appendages (45, 46). During muscle development in chondrichthyans, both appendicular and body wall musculature derive from epithelial extensions of the ventral dermomyotome (47, 48). DP312 labeling presented here in *Scyliorhinus* shows a clean boundary between labeled mesenchyme derived from the DM and unlabeled mesenchyme of presumed lateral plate origin at both fin and interfin levels (Fig. 4). The LPM remains as a mesenchymal layer between the ectoderm and the advancing myotome, such as in the axolotl. Studies of certain hypaxial body wall muscles in pearlfish (49) and the experimental induction of ectopic fin field markers in zebrafish (11) indicate the possibility of this condition in the trunk of fish embryos, although the LPM has not yet been mapped in an actinopterygian. The lateral somitic frontier (50) is a cryptic lineage boundary between somitic vs. LPM, here approximated by DP312 expression in shark and grafted GFP-positive tissues in chimeric axolotls. We conclude that there is a persistent somatopleure in the body wall of both these gnathostomes, which is seen in amniotes. In contrast, our cell labeling data provide evidence that the frontier in lamprey is displaced to the ventral midline of the body wall as the somatopleure is disrupted by growth of the somites.

Relevance to Classical Theories for Paired Fin Origins. The fin/limb buds of all gnathostomes studied arise as outgrowths of the somatopleure, and the skeletal and connective tissue cells of the paired appendages derive from the LPM. Our proposal that the somatopleure is eliminated in lamprey fuels hypotheses about the early history of the LPM and provides an embryological context for focusing questions on the initial conditions necessary for the evolution of the appendicular system. If the lamprey condition is primitive for vertebrates, a comparison of lamprey, cat shark, axolotl, and amniotes would suggest that a persistent somatopleure is a gnathostome synapomorphy (Fig. 6) and that this innovative persistence of somatic LPM external to the myotome was a key early step in the evolution of the embryonic field that ultimately produced paired fins. Advances in molecular genetic tools for lamprey as well as comparative studies of body wall formation in myxinids will further test the polarity of this vertebrate character suite.

One model of paired fin origins suggested by our data is that a persistent somatopleure arose continuously along the flank from the branchial region to the cloaca. This novel LPM domain may have carried an Hox code shared with the regionalized gut (5), presaging the localization and differentiation of pectoral and pelvic potential. Although such a model invokes aspects of the fin fold hypothesis, it does not require the presence of a continuous lateral fin per se. Alternatively, the somatopleure may have initially persisted in proximity to the gills, established a pectoral fin, and subsequently, spread posteriorly to the pelvic level. The latter model is equally supported by our data and has affinities for variations on the gill arch hypothesis (1, 7).

Fossil data support the early and singular appearance of pectoral fins (7, 22), although some authors argue for evidence of ventrolateral fin folds in fossil agnathans (reviewed in ref. 51). Consideration of the advent of a persistent somatopleure in the body wall of ancestral gnathostomes could suggest new interpretations of transitional forms. Many stem agnathans possess lateral fin-like structures that vary in size, number, and position along the flank, and there is debate about their homology with the paired fins of gnathostomes. Using the embryological framework (50) applied here, Johanson (52) recently speculated that these problematic fins are primaxial, consistent with absence of a lateral plate contribution and lack of homology to gnathostome paired fins.

As noted earlier, molecular studies indicate that preexisting gene regulatory networks were co-opted to pattern the fin/limb field. Our embryological data suggest that molecular events provoking mechanistic changes in the relationship between the advancing dermomyotome and the ectoderm in a vertebrate lineage with a previously primaxial body wall could generate a persistent somatopleure with the potential to harbor abaxial structures. We suggest that stem gnathostomes developed a localized expansion of the somatopleure (Fig. 6) in proximity to the nephric ridge at the head–trunk interface. This embryological event was likely induced by molecular signaling between ectoderm and mesoderm, provoked by the partial activation or cooption of genetic networks already established in the gill or heart fields. Such hypotheses can be pursued through comparative molecular studies aimed at testing the source, sequence, and extent of genetic redeployment, resulting in the dramatic morphological innovation of the paired appendages.

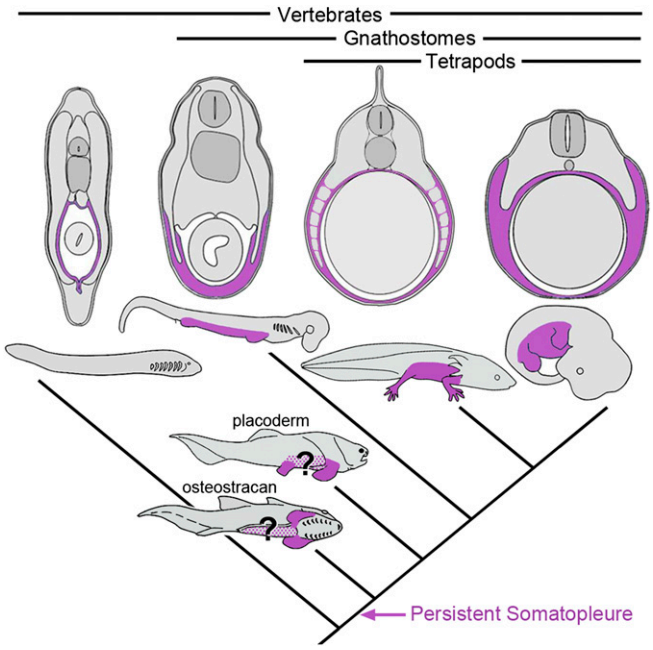

Fig. 6. Evolution of the persistent somatopleure. Simplified vertebrate phylogeny with schematic, midtrunk cross-sections through (left to right) lamprey, shark, axolotl, and amniote embryos. Somatic LPM contributions to the body wall are purple. Somatopleure persistence is a gnathostome synapomorphy. The distribution of somatopleure in fossil taxa is hypothesized (purple stippling). In an osteostracan (ventrolateral view), the somatopleure would correspond to the position of the pectoral fins and may have extended posteriorly, coincident with the hypothetical ventrolateral ridges. In a placoderm, the somatopleure would correspond to the positions of the pectoral and pelvic fins and may have contributed to the interfin trunk. Fossil taxa are modified from ref. 51.

Materials and Methods

Lamprey embryos were staged according to information in the work by Tahara (31). Embryos of *P. marinus* were reared as per the work by Martin et al. (53). Plastic sections for *P. marinus* and *L. japonicum* were generated using JB-4 Plus (EM Sciences) according to the manufacturer's instructions and stained with toluidine blue or H&E.

For immunohistochemistry in lamprey, embryos were fixed in 4% paraformaldehyde. Cryosections were blocked in PBST with 5% (vol/vol) normal goat serum and 2% (vol/vol) bovine serum albumin and incubated overnight with MF20 (1:20 dilution; DSHB) or DP312 (1:20 dilution). AlexaFluor 647 goat anti-mouse IgG2b (Invitrogen) fluorescent secondary was used with MF20. DP312 signal was amplified using a biotinylated secondary (Vector Laboratories) with Streptavidin-Cy5 (SouthernBiotech). Rhodamine-Phalloidin (1:200; Invitrogen) was used to identify skeletal muscle in DP312-labeled sections. Nuclei were counterstained with Sytox Green (Invitrogen). Sections were visualized using a Zeiss LSM510 confocal microscope or Nikon Eclipse E600. Whole-mount specimens were imaged using a Nikon SMZ-U dissecting microscope.

In situ hybridization in *L. japonicum* was performed as described by Sugahara et al. (54) with the Hand probe construct from the work by Kuraku et al. (55).

For fate maps, fixable DiI (Molecular Probes; Invitrogen) was diluted in DMSO (1 μg/μL), loaded into pulled, thin-walled glass capillaries, and pressure injected into somites or LPM (stages 22–24) using a Parker Hannifin General Valve Picospritzer. Embryos were positioned with modeling clay and visualized using a Zeiss Stemi 2000 microscope. The margins of the somites were visible and served as landmarks for somitic injections. For LPM injections, the tip of the capillary was positioned within one somite's width of the lateral somitic margin. When visible, the nephric duct was also used as a landmark. After injection, embryos were raised to stages 25–30 and fixed in 4% PFA. Those embryos with bright DiI labeling in whole mount were cryosectioned and labeled with MF20 or phalloidin.

S. caniculi embryos were staged according to Ballard et al. (39) and labeled with DP312 and goat anti-mouse IgG Cy5 secondary (Jackson Labs) without signal amplification.

GFP and WT embryos of *A. mexicanum* were obtained from the Ambystoma Genetic Stock Center and staged according to the works by Bordzilovskaya et al. (41) and Nye et al. (42). For surgeries, embryos were positioned in 2× Steinberg solution in clay-lined Petri dishes. LPM/Ectoderm or LPM/Ectoderm/Pronephros was isotopically transplanted from stage-matched GFP donors to WT hosts (stages 23–27) using sharpened tungsten needles and pulled glass capillaries. Grafts were held in place by glass coverslip fragments, and Steinberg solution was replaced with 25% Holtfreter solution. Chimeras were evaluated ∼24 h postoperative for graft incorporation and reared at 18 °C.

Cryosections of axolotl chimeras were labeled for GFP as described above using A6455 (1:500 dilution; Invitrogen) and AlexaFluor 488 goat anti-rabbit IgG. Phalloidin was used to identify skeletal muscle, and nuclei were counterstained with TO-PRO-3 Iodide (Invitrogen).

ACKNOWLEDGMENTS. We thank A. Gillis, M. Cohn, and Roscoff Marine Station for fixed embryos of *Scyliorhinus*. N. Patel provided the DP312. MF20 was from the Developmental Studies Hybridoma Bank developed under the auspices of the National Institute of Child Health and Human Development (NICHD) and maintained by the Department of Biology at the University of Iowa. This work was supported by the National Science Foundation East Asia and Pacific Summer Institutes and Sigma Xi (F.J.T.), NICHD Grant R03 HD060062, National Science Foundation Grant 0920520 (to A.C.B.), the Howard Hughes Medical Institute (to support undergraduate initiatives in life sciences), and Wesleyan University.

1. Gegenbaur C (1876) Zur Morphologie der Gliedmaassen der Wirbelthier. *Morph Jahrb* 2:396–420.
2. Thacher JK (1877) Median and paired fins, a contribution to the history of vertebrate limbs. *Trans Conn Acad Sci* 3:281–308.
3. Mivart SG (1879) Notes on the fins of Elasmobranchs, with considerations on the nature and homologies of vertebrate limbs. *Trans Zool Soc Lond* 10(10):439–484.
4. Balfour FM (1881) On the development of the skeleton of the paired fins of Elasmobranchii, considered in relation to its bearing on the nature of the limbs of the Vertebrata. *Proc Zool Soc Lond* 1881:656–671.
5. Coates MI, Cohn MJ (1999) Vertebrate axial and appendicular patterning: The early development of paired appendages. *Am Zool* 39:676–685.
6. Bemis WE, Grande L (1999) *Mesozoic Fishes 2—Systematics and Fossil Record*, eds Arratia G, Schultze HP (Verlag Dr. Friedrich Pfeil, Munich), pp 41–68.
7. Coates MI (2003) The evolution of paired fins. *Theory Biosci* 122:266–287.
8. Tanaka M, et al. (2002) Fin development in a cartilaginous fish and the origin of vertebrate limbs. *Nature* 416(6880):527–531.
9. Gillis JA, Dahn RD, Shubin NH (2009) Shared developmental mechanisms pattern the vertebrate gill arch and paired fin skeletons. *Proc Natl Acad Sci USA* 106(14):5720–5724.
10. Freitas R, Zhang G, Cohn MJ (2006) Evidence that mechanisms of fin development evolved in the midline of early vertebrates. *Nature* 442(7106):1033–1037.
11. Yonei-Tamura S, et al. (2008) Competent stripes for diverse positions of limbs/fins in gnathostome embryos. *Evol Dev* 10(6):737–745.
12. Abe G, Ide H, Tamura K (2007) Function of FGF signaling in the developmental process of the median fin fold in zebrafish. *Dev Biol* 304(1):355–366.
13. Horton AC, et al. (2008) Conservation of linkage and evolution of developmental function within the Tbx2/3/4/5 subfamily of T-box genes: Implications for the origin of vertebrate limbs. *Dev Genes Evol* 218(11–12):613–628.
14. Kokubo N, et al. (2010) Mechanisms of heart development in the Japanese lamprey, *Lethenteron japonicum*. *Evol Dev* 12(1):34–44.
15. Onimaru K, Shoguchi E, Kuratani S, Tanaka M (2011) Development and evolution of the lateral plate mesoderm: Comparative analysis of amphioxus and lamprey with implications for the acquisition of paired fins. *Dev Biol* 359(1):124–136.
16. Shubin N, Tabin C, Carroll S (1997) Fossils, genes and the evolution of animal limbs. *Nature* 388(6643):639–648.
17. Shubin N, Tabin C, Carroll S (2009) Deep homology and the origins of evolutionary novelty. *Nature* 457(7231):818–823.
18. Janvier P (1996) *Early Vertebrates* (Clarendon, Oxford).
19. Donoghue PC, Forey PL, Aldridge RJ (2000) Conodont affinity and chordate phylogeny. *Biol Rev Camb Philos Soc* 75(2):191–251.
20. Capdevila J, Izpisúa Belmonte JC (2001) Patterning mechanisms controlling vertebrate limb development. *Annu Rev Cell Dev Biol* 17:87–132.
21. Haines L, Currie PD (2001) Morphogenesis and evolution of vertebrate appendicular muscle. *J Anat* 199(Pt 1–2):205–209.
22. Coates MI (1994) The origin of vertebrate limbs. *Dev Suppl* 1994:169–180.
23. Osório J, Rétaux S (2008) The lamprey in evolutionary studies. *Dev Genes Evol* 218(5): 221–235.
24. Shimeld SM, Donoghue PCJ (2012) Evolutionary crossroads in developmental biology: Cyclostomes (lamprey and hagfish). *Development* 139(12):2091–2099.
25. Janvier P (2011) Comparative anatomy: All vertebrates do have vertebrae. *Curr Biol* 21(17):R661–R663.
26. Kusakabe R, Kuraku S, Kuratani S (2011) Expression and interaction of muscle-related genes in the lamprey imply the evolutionary scenario for vertebrate skeletal muscle, in association with the acquisition of the neck and fins. *Dev Biol* 350(1):217–227.
27. Richardson MK, Admiraal J, Wright GM (2010) Developmental anatomy of lampreys. *Biol Rev Camb Philos Soc* 85(1):1–33.
28. Shipley AE (1887) On some points in the development of *Petromyzon fluvatilis*. *Q J Microsc Sci* 27(1887):1–46.
29. Goette A (1890) *Abhandlungen zur Entwicklungsgeschichte der Tiere* (Leopold Voss, Hamburg), Vol 5, pp 1–95.
30. Hatta S (1901) On the relation of the metameric segmentation of mesoblast in Petromyzon to that in Amphioxus and the higher Craniota. *Annot Zool Jpn* 5:43–47.
31. Tahara Y (1988) Normal stages of development in the lamprey, *Lampetra reissneri* (Dybowski). *Zoolog Sci* 5(1):109–118.
32. Fernandez-Teran M, et al. (2000) Role of dHAND in the anterior-posterior polarization of the limb bud: Implications for the Sonic hedgehog pathway. *Development* 127(10):2133–2142.
33. Angelo S, et al. (2000) Conservation of sequence and expression of *Xenopus* and zebrafish dHAND during cardiac, branchial arch and lateral mesoderm development. *Mech Dev* 95(1–2):231–237.
34. Kusakabe R, Kuratani S (2005) Evolution and developmental patterning of the vertebrate skeletal muscles: Perspectives from the lamprey. *Dev Dyn* 234(4):824–834.
35. Devoto SH, et al. (2006) Generality of vertebrate developmental patterns: Evidence for a dermomyotome in fish. *Evol Dev* 8(1):101–110.
36. Davis GK, D'Alessio JA, Patel NH (2005) Pax3/7 genes reveal conservation and divergence in the arthropod segmentation hierarchy. *Dev Biol* 285(1):169–184.
37. Hammond CL, et al. (2007) Signals and myogenic regulatory factors restrict *pax3* and *pax7* expression to dermomyotome-like tissue in zebrafish. *Dev Biol* 302(2):504–521.
38. Vélez-Zuazo X, Agnarsson I (2011) Shark tales: A molecular species-level phylogeny of sharks (Selachimorpha, Chondrichthyes). *Mol Phylogenet Evol* 58(2):207–217.
39. Ballard WM, Mellinger J, Lechenault H (1993) A series of normal stages for development of *Scyliorhinus canicula*, the lesser spotted dogfish *(Chondrichthyes: Scyliorhinidae)*. *J Exp Zool* 267(3):318–336.
40. Nowicki JL, Takimoto R, Burke AC (2003) The lateral somitic frontier: Dorso-ventral aspects of anterio-posterior regionalization in avian embryos. *Mech Dev* 120(2):227–240.
41. Borzilovskaya NP, Dettlaff TA, Duhon ST, Malacinski GM (1989) *Developmental Biology of the Axolotl*, eds Armstrong JB, Malacinski GM (Oxford Univ Press, New York), pp 201–219.
42. Nye HL, Cameron JA, Chernoff EAG, Stocum DL (2003) Extending the table of stages of normal development of the axolotl: Limb development. *Dev Dyn* 226(3):555–560.
43. Durland JL, Sferlazzo M, Logan M, Burke AC (2008) Visualizing the lateral somitic frontier in the Prx1Cre transgenic mouse. *J Anat* 212(5):590–602.
44. Shearman RM, Burke AC (2009) The lateral somitic frontier in ontogeny and phylogeny. *J Exp Zoolog B Mol Dev Evol* 312(6):603–612.
45. Dahn RD, Davis MC, Pappano WN, Shubin NH (2007) Sonic hedgehog function in chondrichthyan fins and the evolution of appendage patterning. *Nature* 445(7125): 311–314.
46. Cole NJ, Currie PD (2007) Insights from sharks: Evolutionary and developmental models of fin development. *Dev Dyn* 236(9):2421–2431.
47. Neyt C, et al. (2000) Evolutionary origins of vertebrate appendicular muscle. *Nature* 408(6808):82–86.
48. Cole NJ, et al. (2011) Development and evolution of the muscles of the pelvic fin. *PLoS Biol* 9(10):e1001168.
49. Windner SE, et al. (2011) Distinct modes of vertebrate hypaxial muscle formation contribute to the teleost body wall musculature. *Dev Genes Evol* 221(3):167–178.
50. Burke AC, Nowicki JL (2003) A new view of patterning domains in the vertebrate mesoderm. *Dev Cell* 4(2):159–165.
51. Wilson MVH, Hanke GF, Märss T (2007) *Major Transitions in Vertebrate Evolution*, eds Anderson JS, Sues H-D (Indiana Univ Press, Bloomington, IN), pp 122–149.
52. Johanson Z (2010) Evolution of paired fins and the lateral somitic frontier. *J Exp Zoolog B Mol Dev Evol* 314(5):347–352.
53. Martin WM, Bumm LA, McCauley DW (2009) Development of the viscerocranial skeleton during embryogenesis of the sea lamprey, *Petromyzon Marinus*. *Dev Dyn* 238(12):3126–3138.
54. Sugahara F, et al. (2011) Involvement of Hedgehog and FGF signalling in the lamprey telencephalon: Evolution of regionalization and dorsoventral patterning of the vertebrate forebrain. *Development* 138(6):1217–1226.
55. Kuraku S, Takio Y, Sugahara F, Takechi M, Kuratani S (2010) Evolution of oropharyngeal patterning mechanisms involving *Dlx* and *endothelins* in vertebrates. *Dev Biol* 341(1):315–323.